XVIII IMEKO WORLD CONGRESS
Metrology for a Sustainable Development
September, 17 – 22, 2006, Rio de Janeiro, Brazil

NEW RESULTS IN MODELLING OF A SURFACE TEMPERATURE CALIBRATION SYSTEM

V. C. Fernicola[2], *A. Frattolillo*[1], *L. Rosso*[2], *P. Vigo*[1],

[1]Dip. di Mecc. Strutture Ambiente e Territorio, Università di Cassino, Cassino, Italy, e-mail frattolillo@unicas.it
[2]INRIM, Torino, Italy, e-mail V.Fernicola@imgc.to.cnr.it

Abstract: A dedicated calibration system for contact surface thermometers was designed and constructed and a thermal fluid dynamic model of the system for simulating the impact of the different influence parameters on the measurement was developed. The paper describes the new results of the comparison between the numerical predictions of the calibration system theoretical model and the experimental values, as obtained from its calibration.

Keywords: calibration, surface temperature, reference standard.

1. INTRODUCTION

Contact surface temperature sensors are widely used in scientific and industrial applications because are simple to use and their measurement is independent from the emissivity of the surface. These sensors are particularly suitable for industrial processes where it is necessary to measure time dependent surface temperatures. The metrological traceability of contact temperature sensors is quite different in Europe. In fact, some countries have developed surface temperature standards in the range 10÷300 °C (France) or up to 500 °C (Germany). Other countries, for instance Italy, still use radiation thermometer as standard to measure surface temperature and a thermostatic liquid bath with a standard resistance thermometer to calibrate the contact surface sensors. Obviously, calibration conditions are quite different from real ones and, therefore, many influence parameters, related to the thermal coupling between surface and sensor (shape of the sensor, surface properties, contact thermal resistance, etc.) and the thermal exchange with the surrounding environment (air temperature, air speed, etc.) should be taken into account in the calibration process.

Errors sources can be generally summarized in two different types: systematic and random. Systematic errors, studied in this work, are related to a known physical reason, and have almost the same value and sign at each measurement, and for this reason they can be corrected using an appropriate algorithm. Obviously, even if the error can be corrected, the uncertainty related to this correction will not be negligible and will have to be considered in the uncertainty propagation law. However, the experimental evaluation of these errors is not quite simple [1-4] and for this reason, several mathematical models, based on simplified assumptions [5-10], have been proposed. In most cases, especially for calibration systems, these models cannot fully explain the phenomena involved.

This work presents a numerical procedure, based on the finite element method [11], for the calculation of the systematic errors due to the interaction between the sensor and the measured surface. Despite the developments of numerical methods, only recently the measurement science has started to think about using these methods [12]. The proposed procedure, once adequately validated, will be used for the design of a calibrating system for contact temperature sensors.

2. SYSTEMATIC ERRORS IN CONTACT TEMPERATURE MEASUREMENTS

Systematic errors in contact temperature measurement can be described according to the available literature [13] as follows: i) undisturbed value T_0: temperature of the reference surface when no sensor is placed on it, and the surface only interacts with the surrounding environment; ii) available value T_S: temperature of the portion of the reference surface where the sensor is placed; iii) realized value T_R: temperature deduced from the electrical signal received by the sensor.

Obviously, the calculation of the undisturbed value of the reference temperature T_0 cannot be separated from the uncertainty of the sensors used for its measurement. These can be pyrometers, to directly measure the reference surface temperature, or two or more sensors placed in the reference body, from which the temperature of the reference surface is extrapolated. In the latter case, the temperature profile distortion due to the sensor placement on the reference surface, may cause a further error (T_E in Fig. 1.b), that is not considered in this work, but will be studied in the future. The interaction between the reference surface and the sensor is sketched in Fig. 1.a. The figure shows the fin effect due to the sensor, and the related distortion of the temperature profile in the solid near the measuring section.

Fig. 1.b shows the qualitative temperature profile along the sensor axis, in the case of undisturbed temperature (green line) and disturbed field (blue line). Furthermore, the red temperature profile represents the effect of the extrapolation of the surface temperature from two points

when the temperature field is disturbed by the sensor. The difference between the undisturbed temperature T_0 and the realized value T_R, not considering the calibration error just mentioned (T_E-T_0), can be considered as the sum of three contributions:

$$\Delta\theta = T_R - T_0 = \Delta\theta_1 + \Delta\theta_2 + \Delta\theta_3 \qquad (1)$$

where $\Delta\theta_1 = T_S - T_0$, is known as the first partial error, and is caused by the deformation of the temperature field due to the sensor; $\Delta\theta_2 = T_{SEN} - T_S$, known as the second partial error, is the difference from the available value caused by the contact resistance between the reference surface and the sensor; and $\Delta\theta_3 = T_R - T_{SEN}$, third partial error, is due to the fact that the sensible element (a resistance or a two-metal junction) in the sensor is placed at a certain distance from the reference surface.

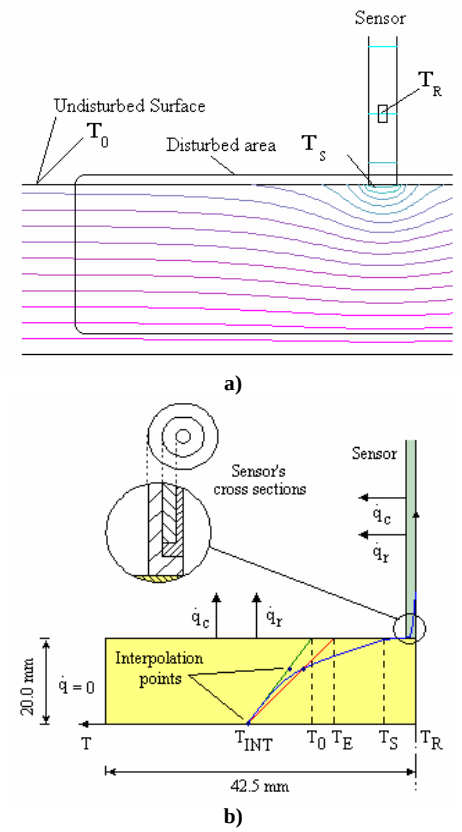

Fig.1. Sketch of temperature distribution in the calibration system with the sensor: (a) isotherms, (b) Computational domain and temperature along the sensors axis

3. NUMERICAL MODEL

The theoretical models developed to study contact temperature errors are generally based on simplified assumptions. In same cases this has led to approximate conclusions, like for instance to believe that, in order to reduce the first partial error, it is necessary to decrease "the heat conducted from the measuring point along the sensor" [9]. However, if the sensor is perfectly isolated, the temperature field would be distorted in the same way, but with an opposite value. The only way to reduce this error would be to design the sensor and its coupling with the surface, so that the sensor's thermal behavior will be the same as that of the environment. In this paper, a numerical procedure for the determination of the first and third systematic (partial) errors in contact temperature calibration systems is proposed. The procedure is based on i) the use of the Finite Element Method (FEM) for the evaluation of the temperature field in both, the system and the sensor, and ii) the calculation of the error due to the presence of sensor.

The numerical procedure is validated by simulating three calibration systems realized by different metrological institutes: the French Laboratiore National d'Essais (BNM) and the Hungarian National Office of Measures (OMH), for which the results are available in literature [3], and the Italian National Institute of Metrological Research (INRIM).

As regard the first two apparatus, the system studied, sketched in Fig. 1.b, with the boundary conditions used for the numerical model, is a cylinder of 85mm of diameter and 20 mm of height, which is kept at the temperature desired by heating from the bottom base. The cylinder has a lateral guard ring and it exchanges heat with the environment (23 °C) from the upper base. In order to reproduce these conditions, the axi-symmetry of the cylinder has been considered, and therefore a bi-dimensional domain was studied; the lateral surface of the cylinder was assumed to be adiabatic, and the bottom base of the cylinder was considered to be at constant temperature, the one that allows the upper base to have the desired temperature.

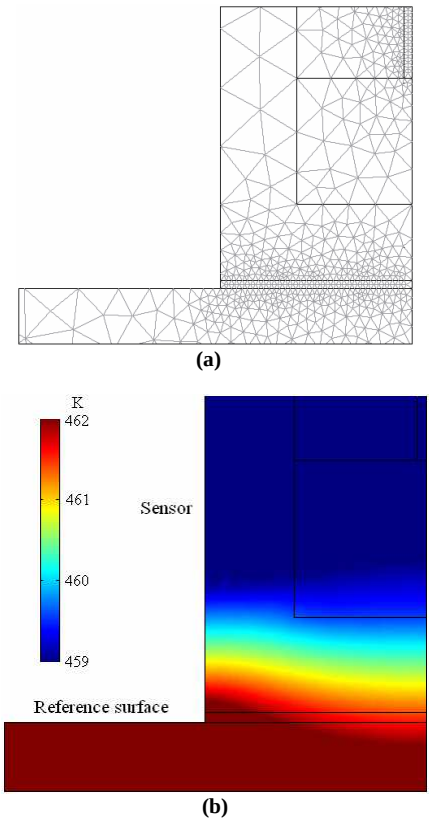

Fig. 2. Numerical solution near the measuring section for one of the problems considered: (a) computational grid; (b) isotherms.

This type of boundary conditions had to be assumed because not enough information was available from the literature about the heating system. The upper surface of the cylinder, as well as the surface of the sensor, exchange by convection and radiation with the surrounding environment. In order to simulate the radiation, configuration factors have been calculated for the surfaces involved, and the environment has been considered as a black body at 23°C. The convection coefficients between the surfaces and the air were calculated on the basis of the relations available in literature [14].

The sensor's geometry has been approximated with an equivalent axi-symmetrical, composed of a spire covered with a metallic material, equivalent to the actual sensor from the point of view of the heat transferred to the environment. This approximation has been already used in literature [6] and is not further explained here.

As regard the INRMI apparatus, an asymmetrical geometry was taken into consideration, and therefore a bi-dimensional domain was studied (Fig. 3). The presence of materials with different thermal conductivities inside the equipment made it necessary to subdivide the domain into the sub-domains outlined in Fig. 3. The grid, which is constituted of about 20,000 triangular quadratic elements, was obtained by using an auto-adaptative procedure available with the code [15]. The mesh was refined where the higher gradients are, as can be seen in Fig. 5b.

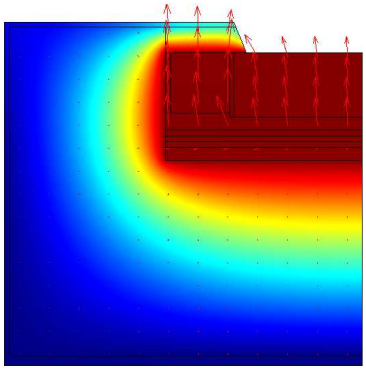

Fig. 3. Bi-dimensional domain for the INRIM complete apparatus.

The operative conditions were simulated by assuming that the lateral surfaces of the apparatus exchange heat with the surrounding environment by means of convection and radiation. In particular, the air around the chamber and the surrounding surfaces was assumed to be at 23°C. The convection coefficients between the surfaces and the air were calculated on the basis of the relationships available in literature [14].

Two further hypotheses were formulated: i) the thermal contact resistances between the reference body, the aluminum cylinder and the heating system were considered negligible; ii) the heating system was approximated with a circular cylinder where an internal heat generation was imposed. The value of the generation was iteratively calculated in order to have the desired undisturbed surface temperature (100, 200, 300 and 400 °C).

4. RESULTS

The results obtained are presented in Figs. 2 and 4. In particular, Fig. 2 shows an example of the mesh used for the calculation (Fig. 2a) and the temperature field (Fig. 2b) around the measurement section, for one of the cases considered. The mesh is automatically adapted on the basis of the local a posteriori error estimate of the solution. The grid is seen to be refined where the highest temperature gradients are. From Fig.2.b it is clear the distortion of the temperature profiles near the measuring section, and their concentration near this section, which is related to the heat transferred through the sensor.

Fig. 4 shows a comparison of the error in the temperature measurement, evaluated experimentally [3] and numerically in this work. It is clear from this figure that when the material used for the reference body is aluminum, the numerical data and the OHM results are not compatible with the BNM values. Because of the lack of further data about the two experimental apparatus in literature, it is not possible to correctly explain these differences. Nevertheless, when the material used for the reference body is steel, the errors calculated numerically are always compatible with the experimental data both for BNM and OHM values.

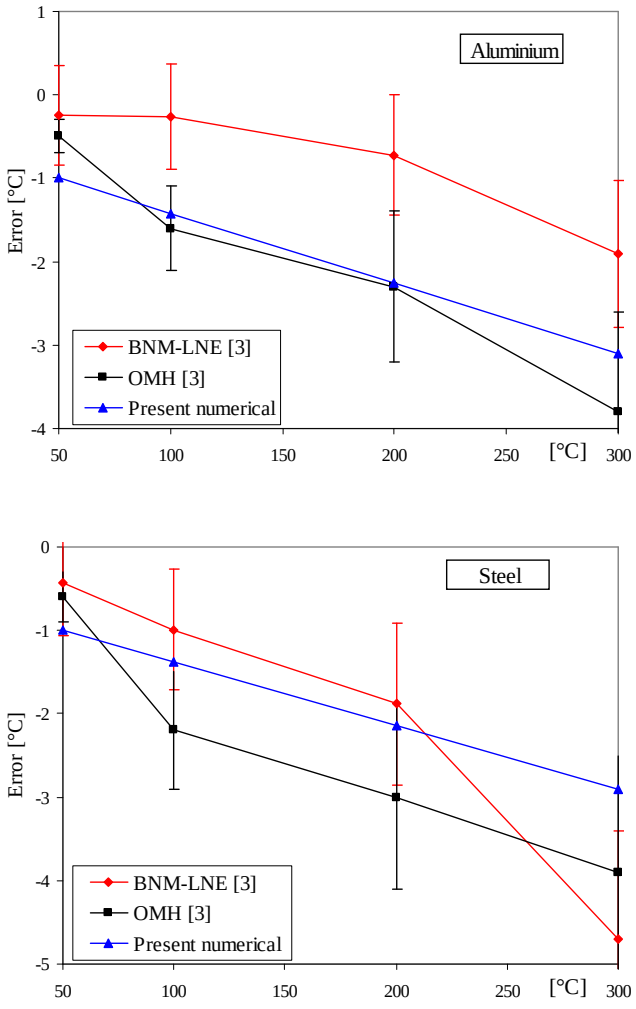

Fig. 4. Comparison of numerical and experimental results of the errors of the BNM and OHM calibration system studied.

As regard the INRIM apparatus, the numerical and experimental results are presented in Figs. 5-6. In particular, Fig. 3a shows the temperature field and the corresponding heat flux vectors inside the measurement apparatus, for one of the cases considered with surface temperature equal to 300 °C. An example of the numerical temperature field near the measurement section, for the above-mentioned case, together with the mesh used for the calculation in the same area, is plotted in Figs. 5a and 5b.

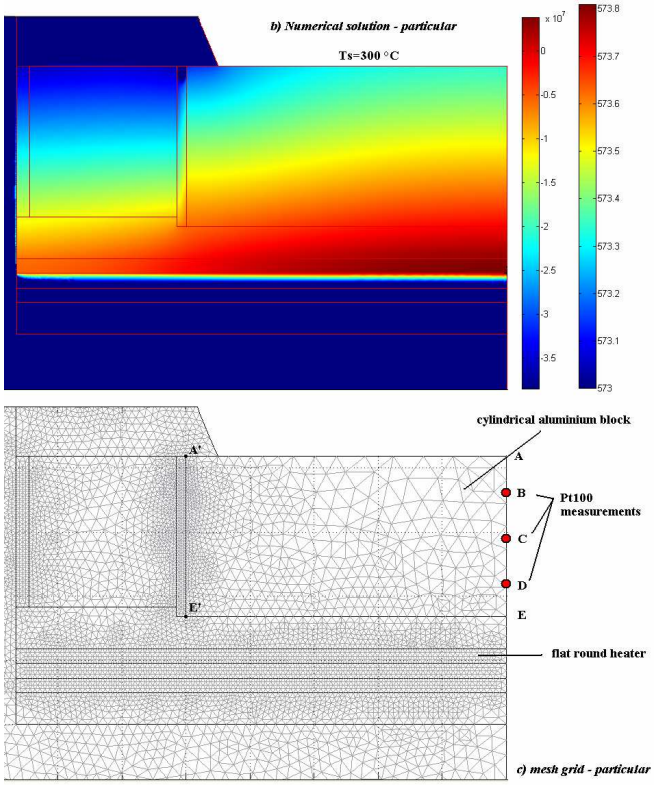

Fig. 5. Numerical simulation for the INRIM cylindrical aluminum block (a) and grid adopted (b) for a surface temperature of 300 °C.

Fig. 6 shows the temperature differences along the upper surface AA' (point A is at 0 mm) and along the AE axis of the cylindrical aluminum block, for different thicknesses of insulating material (5, 10, 20 and 30 mm) at a surface temperature of 100 °C. For the sake of clarity, the temperatures at the different points of the measuring section were plotted with reference to point A' (at x=0, y=50 mm in Fig. 5).

Fig. 7a shows the temperature differences along the upper surface AA' for a 10 mm-thick insulating material and for different surface temperatures. As mentioned above, these temperatures are referred to the temperature of point A'. Lastly, in Fig. 7b the comparison of numerical and experimental results along the AE axis of the cylindrical aluminum block is plotted. In this case, the radial embedding of the three Pt100 used at different depths in the block, the temperature differences along the AE axis refer to the temperature at the experimental reference point B (at x=0, y=6.25 mm in Fig. 5).

The tests carried out for different heights of the cavity showed temperature differences on the reference surface which were always lower then 0.054 °C, for all the range of temperatures investigated. Such differences had a tendency to decrease with the height of the cavity, because the thickness of the insulating material was reduced and its effect decreased. The variation of temperature inside the cylindrical aluminum block showed, instead, an approximate gradient of 0.003 °C/mm, which hardly varied according to the height of the cavity.

The numerical simulation of the prototype developed at the INRIM (with a height of cavity equal to 10 mm) showed a non-uniform temperature distribution lower than 0.221 °C for average surface temperatures lower than 300 °C. The comparison between the experimental data obtained on the cylinder axis and the numerical simulations, was quite interesting. The difference between the experimental and numerical results increased as the temperature of the reference surface rose, but it always stayed below the uncertainty of the sensors utilized (about 0.05 °C), except for the experimental data at 300 °C at the point D in Fig. 5b. In particular, the variation of the temperature inside the cylindrical aluminum block was almost linear according to the numerical simulation, with a slope of 0.003÷0.015 °C/mm, while according to the experimental data it was not always linear and increased with the temperature.

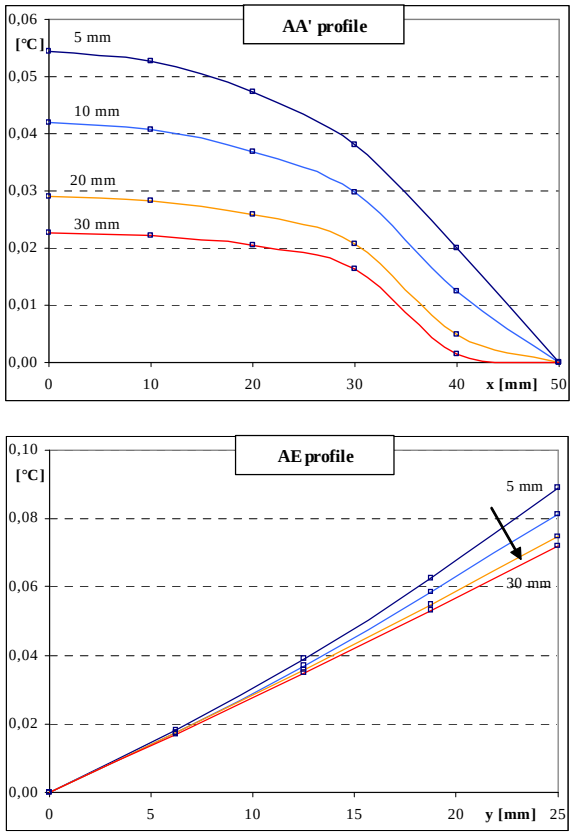

Fig. 6. Temperature differences along the upper surface AA' (point A is at 0 mm) and along the AE axis of the cylindrical aluminum block, for different thicknesses of insulating material and for a surface temperature of 100 °C.

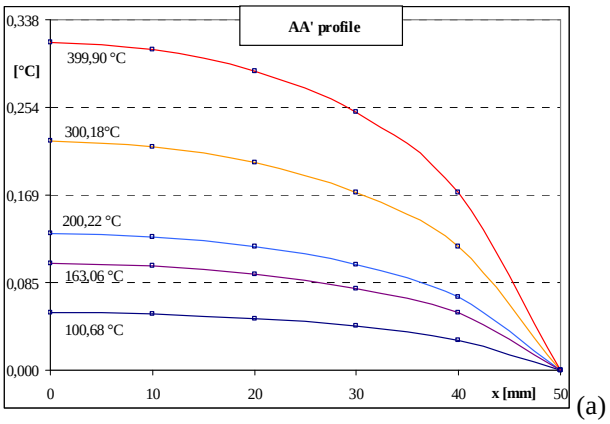

(a)

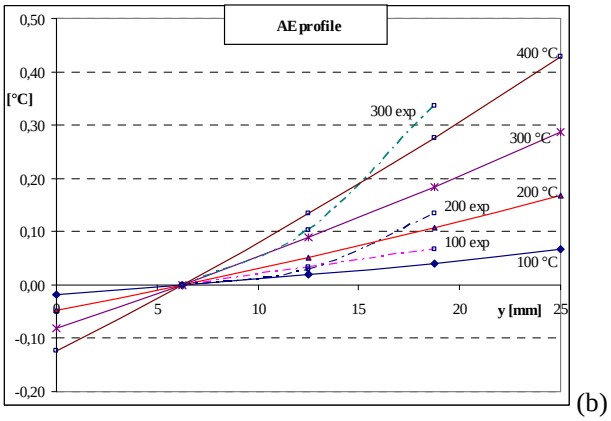

(b)

Fig. 7. (a) Temperature differences along the upper surface AA' (point A is at 0 mm) for a 10 mm-thick insulating material and for different surface temperatures; (b) Comparison of numerical and experimental results along the AE axis of the cylindrical aluminum block.

5. CONCLUSION

The work presents a numerical procedure for the calculation of first and third (partial) systematic errors in contact temperature measurements. The procedure, based on the numerical solution of the temperature field in the reference body and the sensor, is validated by simulating three different calibration systems. The comparison has shown that the procedure can accurately predict the systematic error, as the results obtained proved to be compatible with the experimental results.

This comparison with the INRIM experimental data is quite interesting. It revealed that the differences increased in accordance with the reference surface temperature, but were always lower than 0.015 °C, up to a surface temperature of 300 °C. These differences were probably due to the approximations used in the model.

The numerical model will have to be further developed to reduce its simplifications and to consider more geometrical and thermodynamic details of the prototype, such as the steel clamping system and the uncertainty of the thermodynamic properties of the materials used.

REFERENCES

[1] L. Michalski, K. Eckersdorf and J. Mc Ghee, "Temperature Measurement", 2nd Ed., John Wiley & Sons, 2001.

[2] F. Bernhard, S. Augustin, H. Mammen, K. D. Sommer, E. Tegeler, M. Wagner, U. Demisch and P. Trageser, "Calibration of contacting sensors for temperature measurements on surfaces", Proceedings of Tempmeko 2001, Vol. 1, 19-21 June, Berlin, Germany, 2001.

[3] R. Morice, E. Andràs, E. Devin and T. Kovacks, "Contribution for the calibration and use of surface temperature sensors", Proceedings of Tempmeko 2001, Vol. 2, 19-21 June, Berlin, Germany, 2001.

[4] F. Edler, M. Gorgieva, J. Hartmann and M. Wagner, "Comparison of different methods for the determination of undisturbed surface temperatures", Proceedings of Tempmeko 2001, Vol. 2, 19-21 June, Berlin, Germany, 2001.

[5] D. K. Hennecke and E. M. Sparrow, "Calculating transient wall heat flux from measurements of surface temperature", Int. Journal of Heat and Mass Transfer, Vol. 13, pp. 287-304, 1970.

[6] E. M. Sparrow, "Error estimates in temperature measurement", in Measurement in Heat Transfer, 2nd Ed., edited by E.R.G. Eckert, R.J. Goldstein, Hemisphere Publishing corporation, Washington, 1976.

[7] B. Cassagne, G. Kirsch and J. P. Bardon, "Analyse Teorique des erreurs liees aux transferts de chaleur parasites lors de la mesure d'une temperature de surface par contact ", Int. Journal of Heat and Mass Transfer, Vol. 23, pp. 1207-1217, 1980.

[8] N. R. Keltner and J. V. Beck, "Surface temperature measurement errors", ASME Trans. - Journal of Heat Transfer, Vol. 105, pp. 312-318, 1983.

[9] L. Michalski, K. Eckersdorf and J. Mc Chee, "Surface temperature measurement by portable contact sensors", Proceedings of Workshop on "Surface thermal measurements", 7-9 November, Budapest, Hungary, 1995.

[10] D.Zvizdic, "Modelling of surface temperature measurement errors in vertical natural convection cooled channels", Measurement, Vol. 16, pp. 247-255, 1995.

[11] O. C. Zienkiewicz and R. L. Taylor, "The finite element method", Fifth edition, Butterworth and Heinemann, London, 2000.

[12] M. J. Reader-Harris, C. D. Stewart, A. B. Forbes and G. J. Lord, "Continuous Modelling in Metrology", National Physical Laboratory report, Teddington, Middlesex, UK, 2000 http://www.npl.co.uk/ssfm/download/documents/nel058_2000.pdf.

[13] R. J. Moffat, "Solid and surface temperature measurement with attached and embedded probes", The Western Regional Strain Cage Conference, 1993.

[14] F. P. Incropera and D. P. De Witt, Fundamentals of Heat and Mass Transfer, 5th Ed., John Wiley Text books, 2001.

[15] Femlab v2,3, User manual, Comsol Ab edition, 2000.